Computer simulation study of the global phase behavior of linear rigid Lennard-Jones chain molecules: Comparison with flexible models

A. Galindo[a)]
Department of Chemical Engineering and Chemical Technology, Imperial College London, South Kensington Campus London SW7 2AZ, United Kingdom

C. Vega, E. Sanz, and L. G. MacDowell
Departamento de Química Física, Facultad de Ciencias Químicas, Universidad Complutense de Madrid, Ciudad Universitaria 28040 Madrid, Spain

E. de Miguel and F. J. Blas
Departamento de Física Aplicada, Facultad de Ciencias Experimentales, Universidad de Huelva, 21071, Huelva, Spain

(Received 8 October 2003; accepted 24 November 2003)

The global phase behavior (i.e., vapor-liquid and fluid-solid equilibria) of rigid linear Lennard-Jones (LJ) chain molecules is studied. The phase diagrams for three-center and five-center rigid model molecules are obtained by computer simulation. The segment-segment bond lengths are $L=\sigma$, so that models of tangent monomers are considered in this study. The vapor-liquid equilibrium conditions are obtained using the Gibbs ensemble Monte Carlo method and by performing isobaric-isothermal *NPT* calculations at zero pressure. The phase envelopes and critical conditions are compared with those of flexible LJ molecules of tangent segments. An increase in the critical temperature of linear rigid chains with respect to their flexible counterparts is observed. In the limit of infinitely long chains the critical temperature of linear rigid LJ chains of tangent segments seems to be higher than that of flexible LJ chains. The solid-fluid equilibrium is obtained by Gibbs–Duhem integration, and by performing *NPT* simulations at zero pressure. A stabilization of the solid phase, an increase in the triple-point temperature, and a widening of the transition region are observed for linear rigid chains when compared to flexible chains with the same number of segments. The triple-point temperature of linear rigid LJ chains increases dramatically with chain length. The results of this work suggest that the fluid-vapor transition could be metastable with respect to the fluid-solid transition for chains with more than six LJ monomer units. [DOI: 10.1063/1.1642603]

I. INTRODUCTION

In simple fluids the fluid-solid equilibrium is determined by packing considerations, and freezing can be understood in terms of the freezing of hard spheres. In molecular systems shape, polarity, and flexibility must also be considered. Although it is generally assumed that flexibility is not crucial in determining the fundamental phase behavior of many chainlike fluids, careful analysis reveals that the vapor-liquid critical points of chainlike molecules with different degrees of flexibility are different.[1] It is also well known that systems of rigid nonspherical molecules can exhibit liquid crystalline phase behavior, which is never observed in fully flexible systems. Similarly, it can be expected that flexibility will play an important role in determining the stable solid structure and its thermodynamic properties.

A well-established model to study chainlike molecular systems is one in which the molecules are modeled as chains formed by connected spherical segments. In these models the pair potential between the monomers (either in the same or in different chains) that form the chains is given by a spherical potential. Such models incorporate two essential features: the excluded volume of the chains, and the connectivity between segments. Chain molecules of tangent segments can be considered fully flexible unless bending and torsional potentials are explicitly incorporated. This model is commonly used to represent polymer phase behavior (see Ref. 2 and references therein). Rigid molecules of connected spherical segments can be constructed by fixing the bond angles and internal degrees of freedom, so that the intramolecular energy is constant. In the case of linear molecules liquid crystalline phase behavior can be observed with this model.[3,4] Semiflexible models can also be considered within the same framework by incorporating bending and torsional potentials.

Computer simulations have played a crucial role in the understanding of molecular systems in general, and of the relation of molecular features and macroscopic phase behavior in particular. Dickman and Hall[5] provided the first computer simulation data for the fluid equation of state of fully flexible chains of 4, 8, and 16 tangent hard-sphere segments, which served as a benchmark to test statistical mechanical theories of chain molecules in the late 1980s. Also in the late 1980s, Frenkel and co-workers[6] were able to confirm the predictions of Onsager[7,8] showing that a fluid of hard rods

[a)]Author to whom correspondence should be addressed. Fax ++ (0)20 75945604; Electronic mail: a.galindo@imperial.ac.uk

can exhibit liquid crystalline phase behavior. Liquid crystalline phases of semiflexible[9,10] and rigid chain molecules of tangent hard spherical segments[3,4] were later presented.

Among the theories developed for flexible chains, the thermodynamic perturbation theory (TPT) of Wertheim[11–16] is one of the most successful and widespread. In this theory the properties of the chain system can be obtained provided the properties of the reference monomer system are known; at the first level of approximation (TPT1) the properties are not dependent on the geometrical details of the chains.[15] This prediction was confirmed by computer simulations, which showed that both flexible and rigid chains present similar equations of state.[17] However, a closer look into the behavior of the two systems revealed some differences. Vega *et al.*[18] studied in some detail the effect of flexibility in chain models built from tangent hard-spherical segments. Concentrating on the fluid phases, they noted that the virial coefficients of flexible and rigid hard chains differ significantly. In the intermediate region, as expected,[17] they confirmed that the equations of state of the two models are very similar. At higher densities, but still in the fluid region, linear rigid chain molecules with more than five tangent segments exhibit liquid crystalline phases[3,4,9,10] (as predicted by Flory[19]) which are not seen in fully flexible chain models of any length.

When attractive interactions are incorporated in these models, gas-liquid phase behavior can also be considered. The TPT1 approach of Wertheim has been used to model the fluid-phase equilibria of hard chains with dispersion interactions treated at the mean-field level of van der Waals,[16] Lennard-Jones chains,[20–24] and chains of square-well[25] and Yukawa[26] segments. The approach is widely used to model the phase behavior of chainlike molecules, from *n*-alkanes to polymers, and their mixtures (see Refs. 27 and 28 for recent reviews). As mentioned above, the TPT1 does not take into account flexibility or conformational effects. Based on the fact that the equations of state of rigid and flexible hard chains are very similar in the intermediate density range, it is generally assumed that flexibility does not have a crucial effect on the fluid phase behavior. Recent works have challenged this assumption, however. First, as discussed above, it is clear that if a chainlike molecule is ''stiff'' enough, liquid crystalline phases can be expected to appear, which may interrupt the vapor-liquid phase behavior (see Ref. 29 for an example of the global phase behavior of the Gay–Berne model). Even in the case of semiflexible chains in which liquid crystalline phases are not observed, Sheng *et al.*[1] noted a decrease in the vapor-liquid critical point of semiflexible Lennard-Jones chains of tangent segments. Carrying out computer simulations, they predict a critical temperature 7% lower than that of a flexible chain in the limit of infinite chain length.

In terms of the global phase behavior of chain molecules, it is only recently that solid phases are being considered; the computation of solid-fluid phase transitions of chain molecules by computer simulation is a major undertaking. Empirical rules are frequently used in order to avoid the expensive calculation of the free energy. These techniques have been particularly useful in the study of finite systems and cluster growing in the phase transitions of atomic systems, including Lennard-Jones models (see Ref. 30 and references therein), and homopolymers.[31,32] As in the formation of liquid crystalline phases, it is apparent from the beginning that molecular flexibility plays a crucial role in the stabilization of the solid phase. It was first suggested by Wojciechowski *et al.*[33,34] that the stable structure of a system of flexible molecules of tangent spherical segments should be one exhibiting an fcc close packed arrangement of monomers, but with random bonds, i.e., with no long-range orientational order between bond vectors. Such a structure is referred to as a disordered solid. In the case of semiflexible and rigid molecules, the system cannot adopt a disordered solid structure due to the restrictions imposed by the molecular architecture of the model. The stable structures of rigid and semiflexible chains are expected to be given by layers of molecules arranged in such a way that all the molecules in a layer point in the same direction. In general, molecules in different layers may point in different directions,[35] although differences in free energies of these different arrangements of the layers are expected to be small (at least this was the case for systems of hard dumbbells, where differences in free energies between different solid structures differing only in the orientation of the layers were found to be quite small[35]). One of the possible structures is the so called CP1 solid, in which the molecular axes in all the layers point in the same direction.[35] A similar structure was also considered by Polson and Frenkel[36] when dealing with the fluid-solid transition of semiflexible tangent Lennard-Jones molecules. Polson and Frenkel noted that increasing chain stiffness results in the stabilization of the solid phase (at a fixed temperature the solid-fluid transition pressure is lowered), and that the density gap at the transition is broadened. As we will see later in this work, we observe the same trends in comparing a fully flexible and a linear rigid model of Lennard-Jones (LJ) chains.

Very recently it has been shown that Wertheim's TPT1 can also be applied to the solid phase,[37] allowing the study of fluid-solid equilibrium using the TPT1 for both fluid and solid phases. The fluid-solid equilibria of fully flexible hard-sphere chains,[37] fully flexible hard disks[38] (two dimensions), and fully flexible LJ chains[39–41] have been predicted, yielding good agreement with simulation. A mean-field theory in the spirit of Longuet-Higgins and Widom[42,43] has also been used to model fully flexible hard-chain molecules interacting via mean-field dispersion interactions.[44] Studies of systems with attractive forces have revealed the fact that fully flexible chains present enormous liquid ranges. The predicted ratio of T_t/T_c is of the order of 0.1 for very long chains. For argon this ratio is about 0.55, for propane (which has one of the largest liquid ranges known) it is about 0.23, and for polyethylene it is about 0.35–0.40.[45,46] One may conclude that fully flexible LJ chains present one of the largest liquid ranges that one may obtain for a molecular model. How would the situation change for a rigid model? It is difficult to answer this question. First, it has been shown[47] that, although Wertheim's TPT1 accurately describes the properties of flexible chains in the solid phase, it fails to describe the properties of linear rigid chains in the solid phase. Therefore theoretical predictions of the phase diagram of linear rigid chains

are not available. Vega and McBride,[47] and more recently Blas *et al.*[48] implemented an empirical scaling that describes well the properties (equation of state and free energy) of hard linear chains in the solid phase. When this theoretical description is used in combination with a mean-field term (following Longuet-Higgins and Widom[42]) for the case of linear rigid chains, the predicted T_t/T_c ratio is seen to increase for increasing chain length, causing the vapor-liquid equilibrium to become metastable with respect to freezing for long chains. This is a surprising prediction that was one motivation for this work. Although theories of stiff macromolecules have suggested that the nematic-isotropic transition may preempt the vapor-liquid phase transition, this has not yet been confirmed. In a recent work by Ivanov *et al.*[49] a wide density difference is seen between the nematic and isotropic phases, which points toward the suppression of the vapor-liquid-nematic triple point

Our aim in this paper is to study the phase diagram of linear rigid LJ chains to illustrate the similarities and differences between flexible and linear chains, both for the vapor-liquid equilibrium and for the fluid-solid equilibrium. We will check whether the T_t/T_c ratio increases with increasing chain length, as predicted by the theory recently proposed.[48] In addition, we hope that the simulation data provided here will be useful in the development of theoretical treatments for these systems.

II. SIMULATION DETAILS

We consider Lennard-Jones model chain molecules formed by m identical Lennard-Jones sites (monomers) of diameter σ and dispersive energy ϵ. The molecules are modeled as linear and rigid with segment-segment bond distances $L=\sigma$ (meaning that chains of tangent segments are considered).

The pair interaction between two molecules is given by

$$u(1,2)=\sum_{i=1}^{m}\sum_{j=1}^{m}4\epsilon\left[\left(\frac{\sigma}{r_{ij}}\right)^{12}-\left(\frac{\sigma}{r_{ij}}\right)^{6}\right], \tag{1}$$

where r_{ij} is the distance between site (monomer) i of molecule 1 and site j of molecule 2. Since the model is rigid the intramolecular energy is constant, and we set it to zero. Therefore the internal energies reported here are due only to intermolecular interactions (and not to intramolecular interactions). In this work we carry out computer simulations for systems of linear rigid LJ chain molecules of length $m=3$ (3CLJ) and $m=5$ (5CLJ).

As in previous work,[40] the global phase diagrams for the systems of interest are determined using various simulation techniques. Before describing the details of each of the techniques it is useful to note that in all the simulations performed the site-site LJ pair potential is truncated at $r_c=2.5\sigma$, and that long-range corrections are added to all the computed thermodynamic properties (internal energy, pressure, and chemical potential) by assuming that the site-site pair correlation function is equal to unity beyond the cutoff.[50] A cycle is defined as a trial move per particle (displacement of the center of mass and/or molecular rotation), and a trial volume change. In the case of the Gibbs ensemble simulations a cycle also includes N_{ex} attempts to exchange particles between the boxes. Throughout this work we use reduced units, so that $T^*=T/(\epsilon/k_B)$, $\rho^*=\rho\sigma^3=(N/V)\sigma^3$, $P^*=P/(\epsilon/\sigma^3)$, and $U^*=U/(N\epsilon)$.

A. Vapor-liquid equilibria

The vapor-liquid phase equilibria of a number of flexible LJ chain molecules with tangent segments have been studied previously. The two-center ($m=2$) system has been studied by Dubey *et al.*[51] and Stoll *et al.*,[52] and recently by some of us.[40] Blas and Vega[23,53] presented data for the flexible system with $m=3$, obtained by carrying out Gibbs ensemble Monte Carlo (GEMC) simulations.[54] Escobedo and de Pablo[55] used the GEMC technique with a configurational bias to study systems of LJ flexible chains of 4, 8, 16, and 32 monomers. Longer chains have been studied by Sheng *et al.*,[56] who used the $NPT+$test particle method to obtain the vapor-liquid phase diagrams of polymerlike LJ flexible chains of 20, 50, and 100 tangent segments.

The phase diagram of linear rigid LJ chain molecules has been considered previously only by Perera and Sokolic for molecules with a reduced bond length $L^*=0.505$.[57] The case of ''tangent'' linear rigid LJ chains with $L^*=1$ has not been considered previously (to the best of our knowledge). Hence, we carry out standard GEMC calculations to determine the vapor-liquid coexistence of the two systems of interest here, which will be used for comparison with the flexible ones. At each temperature T^*, initial configurations for the gas and liquid phases are generated by first equilibrating two subsystems (each containing 500 molecules) at the given T^* and with initial vapor and liquid densities close to the expected coexistence values. Constant-volume NVT Monte Carlo simulations are carried out in this equilibration stage, consisting of approximately 10 000–20 000 cycles. The resulting configurations are subsequently used as starting configurations for the Gibbs ensemble run, which consisted of 50 000 equilibration cycles and 50 000 cycles for collecting averages. The coexistence densities, internal energies, pressures, and chemical potentials for each of the temperatures considered are presented in Tables I (linear rigid 3CLJ) and II (linear rigid 5CLJ). The number of particle exchanges and the probabilities of insertion are also presented in the tables. As can be seen, at low temperatures the probability of transferring particles between the two subsystems becomes extremely low, and the Gibbs ensemble technique is found impracticable. Reliable estimates of the coexistence liquid densities at low temperatures can instead be obtained by carrying out NPT simulations at zero pressure. These are presented in Table III for the $m=3$ (3CLJ) and $m=5$ (5CLJ) systems. The procedure is expected to be most accurate at the lowest temperatures, but it can be seen that even at the highest temperature considered the errors are less than 0.1% as compared to the GEMC results of Tables I and II.

The critical temperatures T_c^* and densities ρ_c^* are obtained using the simulation results for the vapor and liquid coexistence densities and the relations

$$\rho_l^*-\rho_v^*=A(T^*-T_c^*)^{\beta} \tag{2}$$

and

TABLE I. Vapor-liquid coexistence properties for linear rigid LJ chains with bond length $L^*=1$ and chain length $m=3$ obtained from Gibbs ensemble Monte Carlo simulations for systems containing initially 500+500 molecules. $T^*=kT/\epsilon$ is the reduced temperature, $\rho^*=\rho\sigma^3$ the reduced number density of molecules, $U^*=U/N\epsilon$ the reduced residual internal energy per particle, $P^*=P\sigma^3/\epsilon$ the reduced pressure, and $\mu^*=\mu/\epsilon$ the reduced chemical potential. The reported pressures and chemical potentials refer to values in the vapor phase (these values are equal to the corresponding values in the liquid phase within the statistical uncertainties). The probability of transferring a particle between the two boxes "Prob" and the number of insertion attempts N_{ins} are also given.

T^*	ρ_v^*	ρ_l^*	U_v^*	U_l^*	P^*	μ^*	Prob	N_{ins}
2.05	0.042(4)	0.133(9)	−2.5(2)	−6.8(4)	0.0478(18)	−8.48(4)	0.03603	250
2.04	0.042(4)	0.142(5)	−2.5(2)	−7.2(2)	0.0470(19)	−8.46(4)	0.02822	350
2.02	0.037(2)	0.145(7)	−2.27(14)	−7.3(3)	0.0431(15)	−8.47(3)	0.02467	500
2.00	0.034(2)	0.152(4)	−2.13(14)	−7.68(19)	0.0408(12)	−8.47(3)	0.01884	600
1.98	0.0300(13)	0.159(3)	−1.93(8)	−8.04(15)	0.0373(10)	−8.48(2)	0.01506	550
1.95	0.0278(18)	0.165(3)	−1.83(11)	−8.36(16)	0.0347(12)	−8.47(3)	0.01225	700
1.90	0.0213(15)	0.175(3)	−1.46(10)	−8.87(18)	0.0283(13)	−8.52(4)	0.00784	800
1.85	0.0169(7)	0.185(2)	−1.20(5)	−9.41(11)	0.0231(7)	−8.55(2)	0.00473	900
1.80	0.0131(6)	0.192(2)	−0.97(4)	−9.86(12)	0.0184(6)	−8.63(3)	0.00305	1000
1.75	0.0096(5)	0.1987(18)	−0.74(4)	−10.25(10)	0.0139(6)	−8.76(4)	0.00205	1250
1.70	0.0079(3)	0.2071(16)	−0.63(2)	−10.76(9)	0.0113(3)	−8.78(2)	0.00120	1500
1.65	0.0063(3)	0.2137(16)	−0.52(2)	−11.16(10)	0.0090(3)	−8.81(3)	0.00071	2000
1.60	0.00467(19)	0.2201(14)	−0.40(2)	−11.57(9)	0.0067(2)	−8.93(3)	0.00042	2500
1.55	0.00361(19)	0.2260(13)	−0.324(19)	−11.96(9)	0.0051(2)	−9.00(4)	0.00024	3000
1.50	0.00278(13)	0.2325(15)	−0.261(17)	−12.39(10)	0.00386(17)	−9.05(4)	0.00013	7500

$$\frac{\rho_l^*+\rho_v^*}{2}=B+CT^*, \tag{3}$$

where ρ_l^* and ρ_v^* are the liquid and vapor coexistence densities at temperature T^*, A, B, and C are constants, and β is the corresponding critical exponent; a value $\beta=1/3$ was assumed here. The critical pressure P_c^* is obtained using the relation

$$\ln P^*=a+bT^*, \tag{4}$$

where P^* is the saturation pressure at temperature T^*, and a and b are constants.

The vapor-liquid critical conditions of the linear rigid LJ chains with $m=3$ are found to be $T_c^*=2.081\pm0.016$, $P_c^*=0.060\pm0.017$, and $\rho_c^*=0.089\pm0.004$ (where ρ^* is the molecular number density). The critical conditions of the system with rigid chains of length $m=5$ are $T_c^*=2.49\pm0.06$, $P_c^*=0.034\pm0.012$, and $\rho_c^*=0.046\pm0.009$.

B. The solid phases

The simulation details regarding the solid phase are similar to those of previous work[35,39,40,58] and hence we discuss here only the main features. In this work the ordered solid CP1 structure is considered, as was done by Sanz *et al.*[41] for LJ rigid chains. In the CP1 structure all molecules of a layer point in the same direction, and all layers point in the same direction. The monomers of the molecules form an fcc close packed structure at the "close packing" density. In the case of the system with $m=3$, $N=400$ molecules are used, by arranging four layers of 100 molecules each. In the case of the model with $m=5$, $N=288$ molecules are used by arranging two layers of 144 molecules each. Since the resulting boxes are noncubic, the Rahman–Parrinello[59] modification of the constant-pressure *NPT* Monte Carlo technique is used in order to allow for nonisotropic changes in the simulation box shape.[60] The simulations were started from configurations at very high pressures, where the density is close

TABLE II. Vapor-liquid coexistence properties for linear rigid LJ chains with bond length $L^*=1$ and chain length $m=5$ obtained from Gibbs ensemble Monte Carlo simulations. Reduced quantities are defined as in Table I.

T^*	ρ_v^*	ρ_l^*	U_v^*	U_l^*	P^*	μ^*	Prob	N_{ins}
2.475	0.0217(14)	0.069(5)	−3.5(2)	−9.3(6)	0.0304(10)	−11.86(3)	0.02032	600
2.450	0.0185(14)	0.074(4)	−3.1(2)	−10.0(4)	0.0274(11)	−11.89(3)	0.01590	700
2.425	0.0188(10)	0.083(3)	−3.19(18)	−11.1(4)	0.0269(10)	−11.82(3)	0.00966	800
2.400	0.0152(8)	0.084(3)	−2.65(13)	−11.3(4)	0.0235(8)	−11.89(3)	0.00855	800
2.375	0.0137(10)	0.089(2)	−2.44(17)	−11.9(3)	0.0216(9)	−11.91(3)	0.00597	1000
2.350	0.0123(4)	0.092(2)	−2.22(7)	−12.4(3)	0.0198(4)	−11.922(18)	0.00423	1000
2.325	0.0114(5)	0.0956(18)	−2.11(10)	−12.9(3)	0.0184(6)	−11.92(3)	0.00321	1200
2.300	0.0094(4)	0.098(2)	−1.78(8)	−13.2(3)	0.0159(5)	−12.02(2)	0.00268	1200
2.275	0.0089(5)	0.101(2)	−1.71(10)	−13.6(3)	0.0149(6)	−12.00(3)	0.00186	1250
2.250	0.0076(3)	0.1028(17)	−1.50(6)	−14.0(2)	0.0131(4)	−12.08(2)	0.00138	1000
2.200	0.0061(3)	0.1086(16)	−1.23(8)	−14.9(2)	0.0107(4)	−12.15(2)	0.00078	2000
2.150	0.0051(3)	0.1131(16)	−1.07(7)	−15.6(2)	0.0089(5)	−12.17(5)	0.00045	5000
2.100	0.00392(10)	0.1182(13)	−0.86(3)	−16.4(2)	0.00700(16)	−12.29(2)	0.00022	10000

TABLE III. Density ρ^* and residual internal energy (per particle) U^* in the liquid phase as obtained from *NPT* Monte Carlo simulations at zero pressure for linear rigid LJ chains with $m=3$ and $m=5$.

m	T^*	ρ^*	U^*
3	1.50	0.2324(16)	−12.39(10)
3	1.45	0.2378(16)	−12.76(10)
3	1.40	0.2437(18)	−13.17(12)
3	1.35	0.2487(16)	−13.52(10)
3	1.30	0.2549(13)	−13.93(9)
3	1.25	0.2597(14)	−14.32(10)
3	1.20	0.2653(17)	−14.74(12)
3	1.15	0.2708(13)	−15.16(10)
3	1.10	0.2755(13)	−15.53(10)
3	1.05	0.2808(10)	−15.94(7)
5	2.10	0.1178(16)	−16.3(2)
5	2.05	0.1217(15)	−17.0(3)
5	2.00	0.1276(15)	−18.1(2)
5	1.95	0.1311(14)	−18.7(2)
5	1.90	0.1366(11)	−19.7(2)
5	1.85	0.1397(11)	−20.31(18)
5	1.80	0.1505(13)	−22.56(3)

to the close packing limit (no true close packing can be defined when a soft potential such as the LJ is used, but the reduced number density of the hard-sphere model at close packing can be used as a good starting point), and were expanded to lower densities by performing *NPT* simulations at slowly decreasing pressures. A typical run of the solid phase involved 40 000 equilibration cycles followed by 40 000 cycles for obtaining equilibrium properties. Some representative simulation results for the solid phase of the models with $m=3$ and $m=5$ are presented in Table IV.

In order to determine the fluid-solid equilibrium, the free energy of the fluid and solid phases must be calculated. The free energy A of the fluid phase at density ρ can be obtained by thermodynamic integration along an isotherm:

$$\frac{A(\rho,T)}{Nk_BT}=[\ln(\rho\sigma^3)-1]+\int_0^{\rho}\frac{[Z(\rho',T)-1]}{\rho'}d\rho', \qquad (5)$$

where Z is the compressibility factor. In this equation, the first term on the right-hand side stands for the ideal gas contribution to the free energy (we have arbitrarily set the de Broglie wavelength to σ), and the rest is the residual part. Following this expression, the free energies of the fluid phase

TABLE IV. *NPT* Monte Carlo simulation results for the CP1 solid phase of linear rigid LJ chains at $T^*=4$ with $m=3$ and 5.

m	ρ^*	P^*	U^*
3	0.46938	80	−4.95
3	0.44783	60	−9.63
3	0.41921	40	−13.73
3	0.39952	30	−15.31
3	0.37046	20	−16.14
5	0.27529	60	−18.23
5	0.26019	40	−25.46
5	0.23777	20	−30.92
5	0.20857	8	−30.47
5	0.20138	6	−29.89

TABLE V. *NPT* Monte Carlo simulation results for the fluid phase at $T^*=4$ for linear rigid LJ chains.

m	ρ^*	P^*	U^*
3	0.00503	0.02	−0.28
3	0.04836	0.2	−2.11
3	0.14235	1	−6.19
3	0.20780	3	−9.09
3	0.25890	7	−10.87
3	0.28815	11	−11.43
3	0.30883	15	−11.45
3	0.32915	20	−11.23
3	0.35900	30	−10.13
3	0.37035	35	−9.21
5	0.00509	0.02	−0.80
5	0.02060	0.08	−2.60
5	0.06905	0.4	−8.23
5	0.09187	0.8	−11.08
5	0.13418	3	−16.55
5	0.14516	4	−17.99
5	0.15385	5	−19.08
5	0.16719	7	−20.60
5	0.17749	9	−21.64

at a temperature $T^*=4$ (supercritical temperature) were obtained via integration of the compressibility factor along the corresponding isotherm. Some representative results of these simulations for the fluid phase are presented in Table V.

In the case of the solid phase, the free energies can be calculated using the Einstein-crystal methodology.[61] The method used here is quite similar to the one described in previous work.[35,39,40,58] Translational and orientational springs are used, with a maximum value (for translational and orientational springs) $\lambda_{\max}=15\,000$ for $m=3$ and $\lambda_{\max}=70\,000$ for $m=5$ (note that the units are k_BT/σ^2 for the translational spring and k_BT for the orientational spring). The free energy calculations were performed at $T^*=4$ using 20 different values of λ in the range $0\leqslant\lambda\leqslant\lambda_{\max}$ and, as before, the length of the runs for the free energy calculations was 40 000 equilibration cycles plus 40 000 averaging cycles. It is important to mention that the shape of the equilibrium unit cell at a given density is slightly different from that at close packing; the free energy calculations were carried out using the equilibrium unit cell at each density. For the CP1 solid structure of the $m=3$ system, we obtained at $T^*=4$ and $\rho^*=0.369\,19$ a free energy value of $A/(Nk_BT)=4.573$; for the $m=5$ system at $T^*=4$ and $\rho^*=0.233\,98$ we obtained $A/(Nk_BT)=3.487$. Using these states as reference, the free energies of the solid phases are obtained as functions of density by thermodynamic integration.

We also carried out *NPT* simulations for the solid phases at very low temperature and zero pressure, since an estimate of the solid densities along the sublimation curve can be obtained in this way. The solid densities along the sublimation curve are presented in Table VI.

C. Gibbs–Duhem simulations

Once the free energies of the fluid and solid phases are known at a fixed temperature ($T^*=4$ in this work), the fluid-solid equilibria can be determined by equating the pressures

TABLE VI. Zero-pressure densities ρ^* of linear rigid LJ chains in the CP1 solid phase as obtained from *NPT* Monte Carlo simulations for $m=3$ and 5.

m	T^*	ρ^*
3	1.05	0.3411
3	1.00	0.3433
3	0.95	0.3452
3	0.90	0.3473
3	0.85	0.3493
3	0.80	0.3512
5	2.05	0.1999
5	2.00	0.2006
5	1.95	0.2017
5	1.90	0.2025
5	1.85	0.2035
5	1.80	0.2044

and chemical potentials of both phases. The results of the fluid-solid equilibrium at $T^*=4$ for the linear rigid 3CLJ and 5CLJ systems are reported in Table VII. In order to obtain the complete fluid-solid coexistence curve in a range of temperatures, the Gibbs–Duhem integration technique can be used. For each chain length studied, initial configurations for the liquid and solid phases are prepared at the equilibrium conditions. In the case of the $m=3$ system, $N=256$ molecules are used in the liquid phase, and $N=300$ (three layers of 100 molecules each) are used for the solid. In the case of the $m=5$ system, $N=256$ molecules are used for the liquid and $N=288$ (two layers of 144 molecules) for the solid.

The Gibbs–Duhem method is implemented carrying out isotropic *NPT* simulations for the fluid phase, and nonisotropic *NPT* simulations for the ordered solid structure, and using a modified version of the Clausius equation (see also Ref. 40), which can be written as

$$\left(\frac{d\ln P}{d\beta}\right)=-\frac{\Delta h}{\beta P\Delta v} \tag{6}$$

where $\beta=1/T$, and Δh and Δv are the enthalpy and volume differences per particle between the fluid and solid phases, respectively. The integration of this equation requires an initial coexistence point (here, the fluid-solid equilibrium results at $T^*=4$ are used; see Table VII), and a simple trapezoidal rule can then be used with a step $\Delta\beta$. Details of the integration technique are similar to those reported previously.[40] As in our previous work,[40] the lengths of the runs used to determine the coexistence pressure for a new temperature were 5000 equilibration cycles and 5000 averaging cycles. Once the coexistence pressure for a new temperature is determined, runs of 30 000+30 000 cycles are used to determine the equilibrium properties at coexistence.

TABLE VII. Coexistence densities, pressures, and chemical potentials at $T^*=4$ used as starting states for the Gibbs–Duhem calculations.

m	T^*	P^*	ρ_l^*	ρ_s^*	$\mu/(k_BT)$
3	4	35.108	0.3699	0.4102	27.75
5	4	6.580	0.165	0.203	9.76

We have typically used a step $\Delta\beta=0.02$ in the integration. The algorithm was checked by implementing this Gibbs–Duhem integration scheme to determine the fluid-solid equilibrium properties of a LJ monomer system, and the results were found to be in good agreement with those of other works.[62,63] The same algorithm was used in a previous work to study the solid-fluid equilibrium of two-center Lennard-Jones (2CLJ) molecules.[40]

III. RESULTS

In this work we consider model chain molecules built from tangent spherical Lennard-Jones segments in order to investigate the effect of molecular flexibility on the phase behavior of these systems. We examine the global phase behavior, including solid-fluid as well as vapor-liquid transitions. We consider at this stage two limiting cases: freely jointed chains and linear rigid chains.

Although it is commonly assumed that molecular flexibility has little effect in terms of the fluid phase behavior, recent work has questioned this.[1] Hence, we start by considering the effect of flexibility on the fluid phase transitions. In Fig. 1(a) the T^*-ρ^* phase diagrams for model systems of chains with three tangent LJ segments are presented. Computer simulations of the fully flexible 3CLJ system were carried out previously by Blas and Vega;[23,53] they report a critical point at $T^*=2.06$ and $\rho^*=0.088$. Here, we have carried out GEMC simulations for the corresponding rigid system (see the previous section for details of the simulations); the critical point in this case is found to be $T_c^*=2.081\pm0.016$, $P_c^*=0.060\pm0.017$, and $\rho_c^*=0.089\pm0.004$. A comparison between the two simulation studies suggests a slightly higher critical temperature value for the rigid system, although this is difficult to confirm given the (relatively) large error associated with our estimation of the critical temperature from computer simulations. Away from the critical point, little difference is observed for the coexistence densities of the two models. As we will see later, the effect of flexibility is more noticeable for larger chains. In Fig. 1(a) the result of a calculation with the TPT1 of Wertheim for Lennard-Jones chains[22,23] is also presented for comparison. The theory gives a very good description of the phase behavior of the system for the entire phase envelope, although larger deviations are seen in the region close to the critical point, as expected from any classical equation of state.

In Fig. 1(b) the T^*-ρ^* phase diagram for LJ chain molecules with $m=5$ tangent segments is presented. We obtained the phase envelope for linear rigid molecules using GEMC simulations (see the previous section), and find the critical conditions at $T_c^*=2.49\pm0.06$, $P_c^*=0.034\pm0.012$, and $\rho_c^*=0.046\pm0.009$. Unfortunately, no simulation data are available for the flexible model. As comparison we have included in the figure the vapor-liquid envelope obtained with the TPT1 of Wertheim. Blas and Vega[53] showed that the approach provides an excellent description of the phase behavior of flexible LJ chain molecules. Assuming that the theoretical calculations represent the phase behavior of the flexible model in the case of $m=5$, we can conclude that a widening of the T^*-ρ^* envelope is seen as a result of an

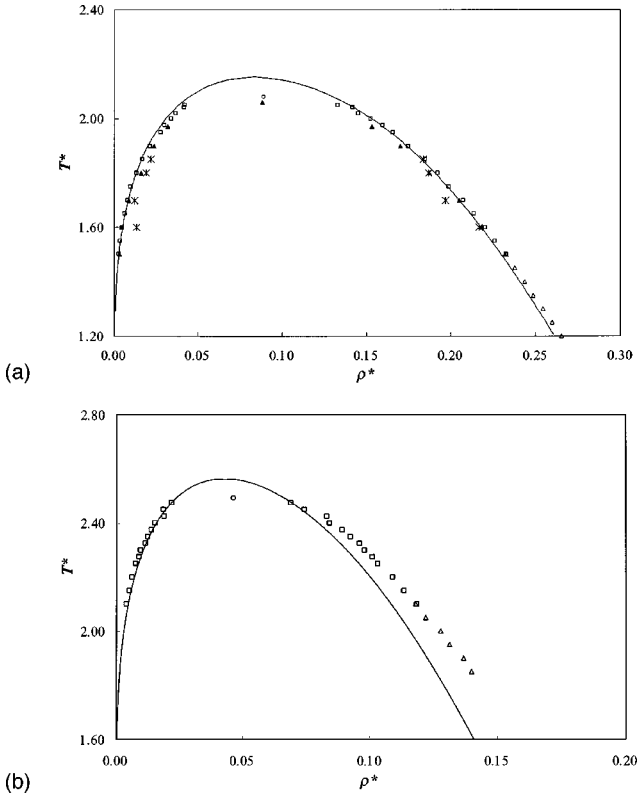

FIG. 1. (a) Vapor-liquid coexistence curve (T^*-ρ^* representation) for 3CLJ model systems with tangent segments from computer simulation (symbols) and predictions from Wertheim's TPT1 (curve). The open squares correspond to the Gibbs ensemble Monte Carlo simulation results obtained in this work for the linear rigid model; the open circle indicates the critical point estimated from the simulation results as described in the main text. The open triangles correspond to the liquid densities obtained in this work using *NPT* Monte Carlo simulations at zero pressure. The closed triangles (Ref. 53) and asterisks (Ref. 23) indicate the Gibbs ensemble data of Blas and Vega for flexible molecules. (b) Vapor-liquid coexistence curve (T^*-ρ^* representation) for 5CLJ model systems with tangent segments from computer simulation (symbols) and predictions from Wertheim's TPT1 (curve). The open squares correspond to the Gibbs ensemble Monte Carlo simulation results obtained in this work for the linear rigid model; the open circle indicates the critical point obtained with the scaling relations given in the text. The open triangles correspond to the zero-pressure NPT calculations. The curve corresponds to the TPT1 predictions, which serve as a model for a flexible system.

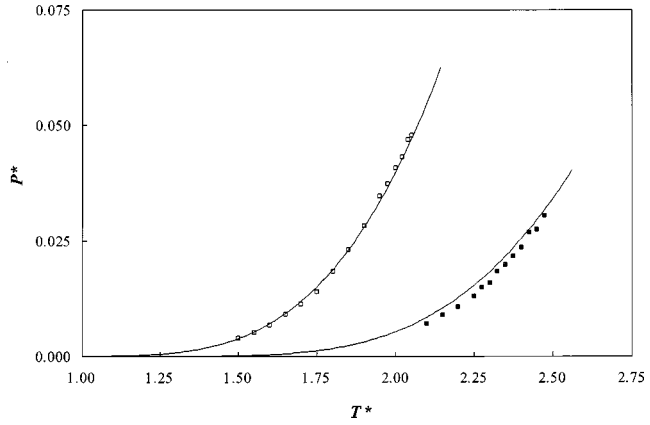

FIG. 2. Vapor pressure curve (P^*-T^* representation) for 3CLJ and 5CLJ model systems with tangent segments from computer simulation (symbols) and predictions from Wertheim's TPT1 (curves). The open squares correspond to the simulations of this work for the rigid 3CLJ system, and the closed squares to those of the 5CLJ. The curves indicate the pressures as calculated with Wertheim's TPT1, which serves as a model for flexible systems.

increased stiffness in the chain. The phase diagram in the P^*-T^* projection is presented in Fig. 2. The vapor pressure curves for the 3CLJ and 5CLJ systems are shown. The simulations carried out in this work for the linear rigid models are compared with calculations using the TPT1 approach of Wertheim, which can be considered as accurately representing a flexible chain model. The flexible and rigid 3CLJ models exhibit vapor pressure curves which are very close, as could be expected given the T^*-ρ^* diagram of Fig. 1(a). In the case of the 5CLJ systems, a slight difference in vapor pressure is noted between the flexible and rigid systems. The results presented in Figs. 1 and 2 seem to suggest that, while little difference is observed in the equations of state of flexible and rigid chains of tangent hard spherical segments,[17,18] a noticeable difference in the vapor-liquid equilibrium is seen when attractive interactions are also involved.

The simulation data for flexible and rigid models for LJ chains with $m=3$ [see Fig. 1(a)] suggest an increase of the critical temperature with increased stiffness. Unfortunately, the comparison presented in Fig. 1(b) cannot confirm this tendency to increase the critical point as the theory does not provide the correct universal critical behavior. In order to examine the effect of flexibility on the vapor-liquid coexistence in terms of the critical temperature it is useful to construct a Schultz–Flory[64] diagram; this is presented in Fig. 3. In this representation a linear relation is obtained between the inverse critical temperature and a function of the number of beads in the model chain. We have used data from the literature for the critical temperatures of the fully flexible chains.[23,53,55,56] As can be seen in Fig. 3, the critical temperature of linear rigid chains with $m=3$ and 5 seems to be higher than that of fully flexible chains. One may speculate on the behavior of both systems for infinitely long chains.

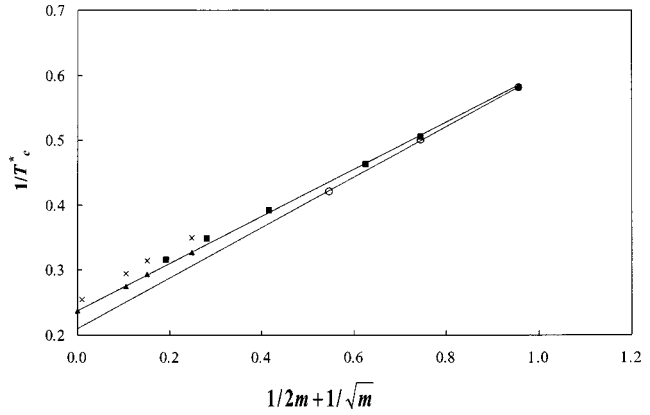

FIG. 3. Schultz–Flory diagram comparing the critical temperature of flexible, rigid, and semiflexible models. The open circles correspond to the critical points of linear rigid chain molecules of LJ tangent segments as obtained in this work; the closed symbols represent the critical points of flexible chains of tangent LJ segments as obtained by Escobedo and de Pablo (Ref. 55) (squares) and Sheng *et al.* (Ref. 56) (triangles). The crosses correspond to the critical points obtained by Sheng *et al.* (Ref. 1) for semiflexible chains of tangent LJ segments. The lines are guides to the eye.

TABLE VIII. Fluid-solid coexistence properties obtained using the Gibbs–Duhem integration scheme for linear rigid LJ chain molecules of bond length $L^*=1$ and chain length $m=3$. The initial equilibrium point for the Gibbs–Duhem integration was a state at $T^*=4$ and $P^*=35.108$. ρ_f^* and ρ_s^* are the fluid and solid densities at fluid-solid coexistence, respectively.

T^*	P^*	ρ_f^*	ρ_s^*	T^*	P^*	ρ_f^*	ρ_s^*
4.0000	35.1080	0.3711	0.4102	1.5873	5.1280	0.3112	0.3576
3.7037	30.9665	0.3665	0.4051	1.5385	4.6330	0.3091	0.3561
3.4483	27.4979	0.3606	0.4004	1.4925	4.1736	0.3080	0.3550
3.2258	24.5524	0.3556	0.3963	1.4493	3.7490	0.3065	0.3538
3.0303	22.0125	0.3526	0.3921	1.4085	3.3523	0.3044	0.3525
2.8571	19.7763	0.3500	0.3891	1.3699	2.9813	0.3024	0.3512
2.7027	17.8482	0.3442	0.3855	1.3333	2.6343	0.3012	0.3501
2.5641	16.1452	0.3414	0.3825	1.2987	2.3074	0.2998	0.3493
2.4390	14.6258	0.3387	0.3795	1.2658	2.0034	0.2978	0.3479
2.3256	13.2777	0.3356	0.3770	1.2346	1.7175	0.2940	0.3472
2.2222	12.0702	0.3320	0.3743	1.2048	1.4498	0.2936	0.3463
2.1277	10.9827	0.3305	0.3723	1.1765	1.1965	0.2912	0.3455
2.0408	10.0020	0.3268	0.3697	1.1494	0.9587	0.2878	0.3448
1.9608	9.1088	0.3239	0.3677	1.1236	0.7329	0.2890	0.3441
1.8868	8.2980	0.3231	0.3658	1.0989	0.5202	0.2874	0.3434
1.8182	7.5524	0.3205	0.3639	1.0753	0.3184	0.2849	0.3426
1.7544	6.8717	0.3183	0.3622	1.0526	0.1279	0.2826	0.3421
1.6949	6.2416	0.3166	0.3606	1.0309	0.0011	0.2839	0.3419
1.6393	5.6624	0.3128	0.3592				

The critical point of an infinitely fully flexible chain of LJ tangent segments is found to be $T^*=4.59$ (as suggested by Sheng *et al.*). Extrapolating from the GEMC simulations for linear rigid chains of LJ $m=3$ and $m=5$ tangent segments, the critical temperature of an infinitely long linear rigid chain is found to be $T^*=5.27$; i.e., of the order of 25% higher than that of the flexible model. However, our estimate of the critical temperature of infinitely long linear rigid LJ chains should be treated with caution since molecules with $m=3$ and 5 are certainly too short to yield linear behavior in a Schultz–Flory plot. Simulation data for longer linear rigid chains are needed to establish definite conclusions in this respect. Our present results seem to suggest that the critical point of infinitely long linear LJ chains may be higher than that of the fully flexible model (this is certainly the case for short chains), but more work needs to be carried out to clarify this point completely. It is important to mention also that Sheng *et al.* examined the critical temperature of semiflexible model molecules formed by tangent LJ segments. In their model the bond angle was fixed to the tetrahedral value, and a torsional potential was introduced. They showed that such a nonflexible model yields a critical temperature lower than that of the fully flexible case. In this work we have found the opposite (i.e., a higher critical temperature for the linear rigid model) in comparing to the fully flexible model. This seems to indicate that the way in which chain stiffness is incorporated can affect the critical properties and chemical details of the model (the bond angle in our work is 180° as compared to 109.5° used by Sheng *et al.*). Although, as suggested earlier, it may turn out that the linear rigid chains considered here are too short for the Schultz–Flory plot to be valid. For short chains, the critical temperature of linear rigid chains seems to be lower than that of fully flexible chains. For long chains, we have only an indication that the same may be true, and further work is needed in this respect. As a conclusion of this part of the work, it seems clear that flexibility has a non-negligible effect on the vapor-liquid phase behavior of chains with attractive interactions, and that a number of issues are yet to be resolved.

Let us now turn our attention to the solid-fluid equilibria. In previous work,[39] an extension of the TPT1 of Wertheim was proposed which can be used to model the solid phases of fully flexible chain molecules of LJ tangent segments. The approach provides an excellent description of the global phase behavior of the 2CLJ system,[40] and, although the phase behavior of longer flexible chains has not yet been compared with computer simulation data, it is useful to review here the main findings of the predicted phase behavior of fully flexible LJ chains.[39] The most striking feature is the existence of an enormous fluid range (in the limit of infinitely long chains the ratio T_t/T_c is 0.14). This is due to the fact that the critical temperature of chain molecules increases for increasing chain length, whereas the calculated triple-point temperature remains practically constant; in fact it is seen to decrease slightly for increasing chain length. The stable solid structure for flexible chains of tangent spherical segments is the so-called disordered solid,[33,34] a solid structure in which the spherical segments are arranged in a close packed fcc lattice with no long-range orientational order between bond vectors. The stable solid structure of a system of rigid chains, however, corresponds to an ordered arrangement of layers with the molecular axes of all the molecules in a layer pointing in the same direction (i.e., the CP1 structure). Since the equilibrium solid structure is different for both models, and since the Hamiltonian of both systems is certainly different, one may expect important differences in the fluid-solid equilibrium of both systems.

We have used the Gibbs–Duhem integration technique to obtain the fluid-solid coexistence curve in a range of temperatures (Tables VIII and IX) for linear rigid LJ chain molecules. At low temperatures the solid densities along the sublimation curve can be estimated from the zero-pressure

TABLE IX. Fluid-solid coexistence properties obtained using the Gibbs–Duhem integration scheme for linear rigid LJ chain molecules of bond length $L^*=1$ and chain length $m=5$. The initial equilibrium point for the Gibbs–Duhem integration was a state at $T^*=4$ and $P^*=6.58$. ρ_f^* and ρ_s^* are the fluid and solid densities at fluid-solid coexistence, respectively.

T^*	P^*	ρ_f^*	ρ_s^*
4	6.5800	0.1648	0.2001
3.7037	5.4647	0.1638	0.1994
3.4483	4.5300	0.1615	0.1996
3.2258	3.7296	0.1571	0.1979
3.0303	3.0531	0.1564	0.1964
2.8571	2.4625	0.1516	0.1982
2.7027	1.9504	0.1473	0.1954
2.5641	1.5104	0.1475	0.1982
2.4390	1.1156	0.1437	0.1989
2.3256	0.7697	0.1384	0.1987
2.2222	0.4634	0.1333	0.1990
2.1276	0.1976	0.1278	0.1993
2.0408	0.0067	0.1232	0.1996

simulations presented previously (Table VI). The global phase diagrams obtained from simulation are presented in Figs. 4 (T^*-ρ^* projection) and 5 (P^*-T^* projection). The triple-point temperature can be estimated from the simulation

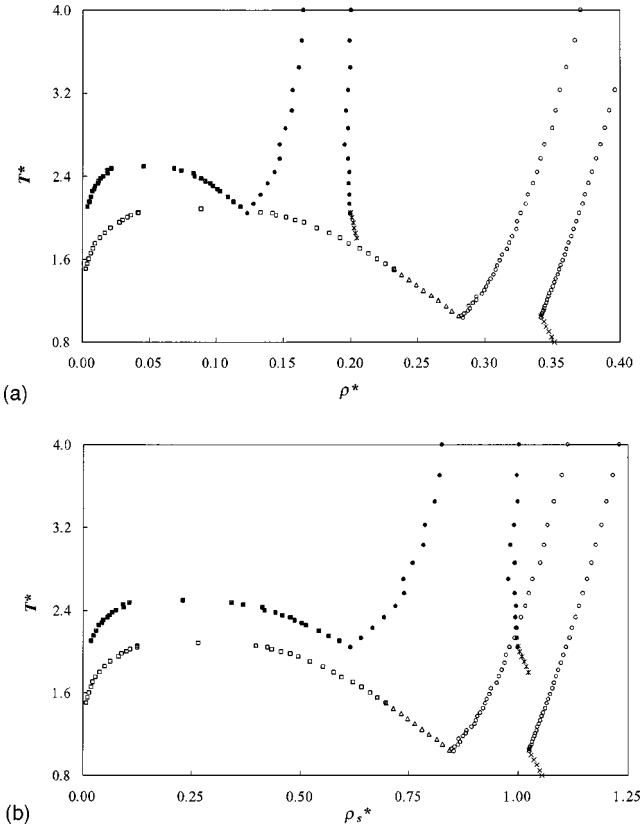

FIG. 4. Global phase diagram in (a) T^*-ρ^* and (b) T^*-ρ_s^* (where $\rho_s^*=\rho^* m$) representations for linear rigid chain molecules of three and five tangent LJ segments as obtained from the simulations of this work. The open symbols correspond to the 3CLJ system and the closed symbols to the 5CLJ system. The squares correspond to the results of GEMC calculations, the triangles to the *NPT* calculations of the liquid phase at zero pressure, the circles to the solid-fluid coexistence densities obtained with Gibbs–Duhem calculations, and the asterisks and crosses to the solid densities obtained with *NPT* calculations at zero pressure.

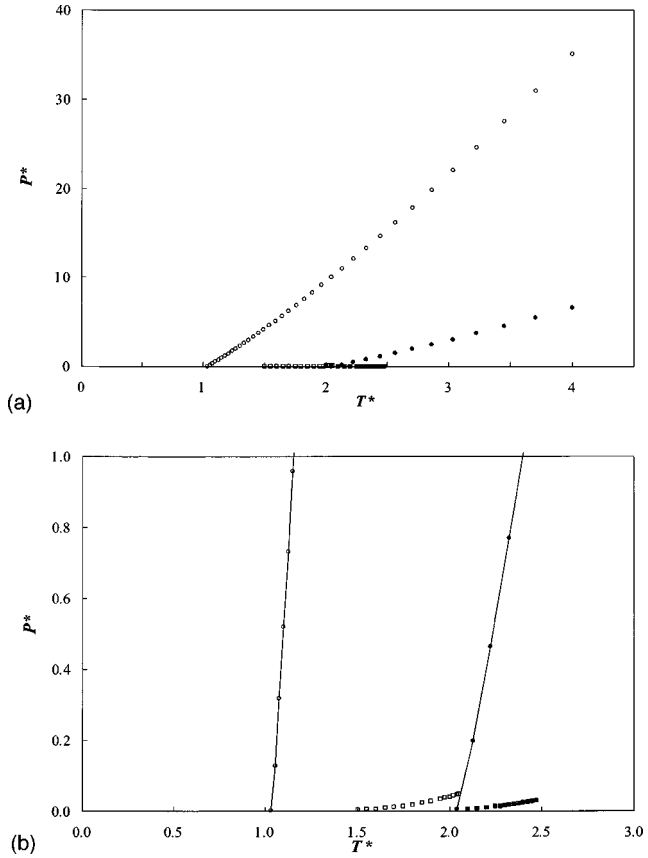

FIG. 5. Global phase diagram in P^*-T^* representation for linear rigid chain molecules of three and five tangent LJ segments as obtained from the simulations of this work. See Fig. 4 for details of the symbols. (b) shows the P^*-T^* projection at low pressures (the lines are guides to the eyes).

results by extrapolating the fluid-solid coexistence temperatures to zero pressure (i.e., the vapor-liquid-solid triple-point pressure is expected to be very small). Conversely, it can also be determined by finding the temperature at which the density of the fluid at zero pressure becomes identical to that of the fluid in the fluid-solid coexistence curve. The triple-point temperatures and densities for the linear rigid 3CLJ system are $T_t^*=1.040$, $\rho_l^*=0.281$, and $\rho_s^*=0.342$. For the linear rigid 5CLJ system these are $T_t^*=2.050$, $\rho_l^*=0.122$, and $\rho_s^*=0.199$. In a previous work the triple point of the 2CLJ system was found[40] to be $T_t^*=0.650$, $\rho_l^*=0.462$, and $\rho_s^*=0.515$ (note that for the 2CLJ the stable solid structure at the triple point is a disordered one). In contrast with the phase behavior of flexible chains, a clear stabilization of the solid phases results from increasing chain lengths in these rigid systems. The triple-point temperature increases dramatically, faster, in fact, than the increase seen for the critical point. As a result, the region of vapor-liquid coexistence decreases. The T_t^*/T_c^* ratio is 0.50 for the chain with three segments, while it is 0.82 for the five-segment chain. By comparison, the fluid range of flexible molecules of similar chain lengths, as predicted by our theoretical approach,[39] is of the order of 0.30. Another indication of the stabilization of the solid phases is the shift toward lower densities in the fluid-solid transition [see especially Fig. 4(b)], and the widening of the density gap. These results are in agreement with

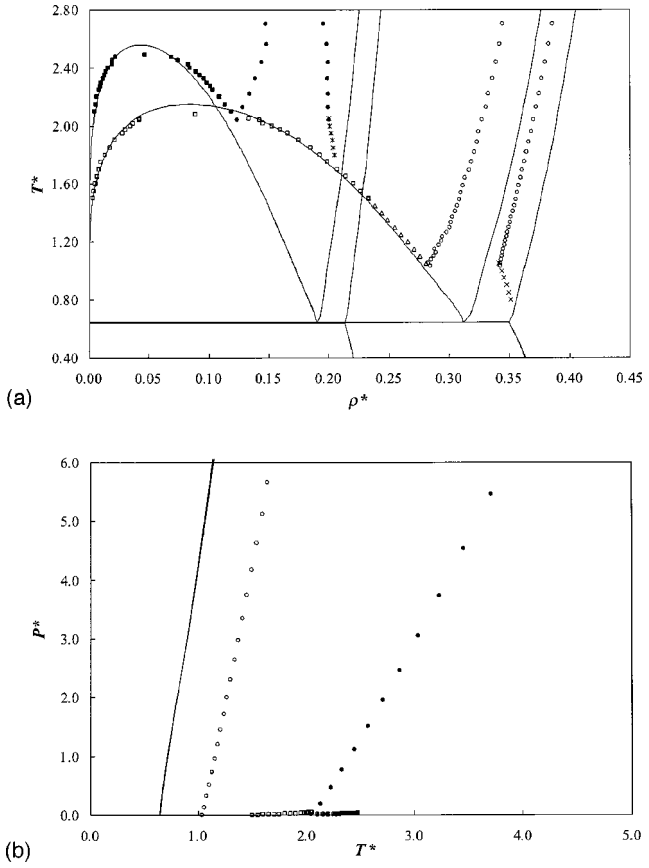

FIG. 6. Global phase diagram in (a) T^*-ρ^* and (b) P^*-T^* representations for linear rigid chain molecules of three and five tangent LJ segments as obtained from the simulations of this work and compared with TPT1 calculations (Ref. 39). The solid lines correspond to the TPT1 calculations for the flexible chains and the symbols to the simulation points of the rigid systems. See Fig. 4 for details of the symbols.

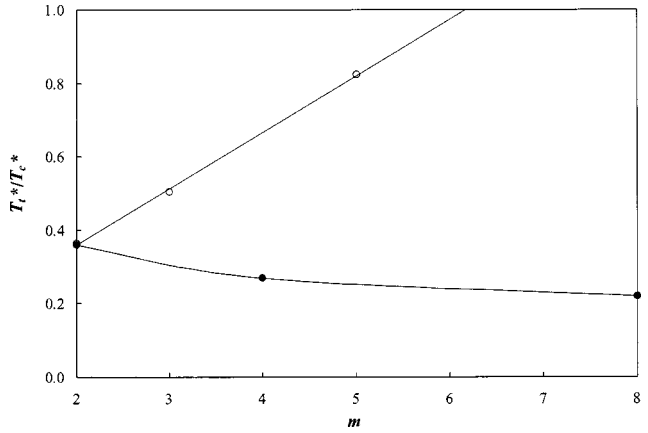

FIG. 7. Sketch of the T_t/T_c ratio for varying chain length in model chains of tangent LJ segments. The open symbols correspond to the ratios for linear rigid molecules as obtained in this work, and the closed symbols to the ratios of flexible molecules as obtained with Wertheim's TPT1 in previous work (Ref. 37). The curves are guides to the eye.

the simulations of Polson and Frenkel.[36] In Fig. 5 the P^*-T^* projections of the phase diagrams as obtained from simulation are shown for the 3CLJ and 5CLJ systems. At a fixed pressure the solid-liquid melting temperature is displaced to higher temperatures for increasing chain length. As before, this corresponds to a stabilization of the solid phase. In Fig. 5(b) the shift of the triple-point temperatures can be better observed. A comparison of the phase behavior of linear and flexible chains can be seen in Fig. 6. The phase behavior of the flexible model is obtained with the TPT1 approach presented in earlier work.[39] It can be clearly seen in Fig. 6 that in the case of the flexible model the predicted triple-point temperature remains practically constant for increasing chain lengths; this leads to the large fluid range seen in the flexible model systems. Using the distance fluctuation criterion for melting and computer simulations, Zhou *et al.*[31,32] noted that the results obtained with clusters of square-well segments and isolated square-well homopolymers are very similar, and suggest that chain connectivity does not affect the solid-liquid equilibrium in the case of freely jointed chains; our TPT1 model seems to lead to the same conclusion. In the rigid systems, however, the marked stabilization of the solid phases results in an increase of the triple-point temperatures and the shrinkage of the fluid range.

It is encouraging to see that the trends highlighted here for the rigid chains confirm the predictions of our theoretical calculations for chains of tangent hard segments interacting via attractive dispersion interactions treated at the mean-field level of van der Waals.[48] In the former work a simple extension of Wertheim's theory is coupled with a scaling argument to take into account the fewer degrees of freedom of a rigid chain (as compared to a flexible chain). As regards the theory, the stabilization of the solid phase with respect to the fluid is explained in terms of this loss of degrees of freedom. It was also suggested that, as a result of the marked increase in the triple-point temperature, the vapor-liquid envelope would be metastable in systems of long rigid chains with attractive interactions. An extrapolation of the values of the T_t^*/T_c^* ratio as obtained from simulation in our present work suggests that chains with more than six segments will not exhibit stable vapor-liquid transitions (see Fig. 7). In the figure the ratios corresponding to flexible LJ chains as predicted by the extension of Wertheim's theory[37] are also shown for comparison. In the flexible systems, the liquid-vapor envelope not only does not become metastable for any chain length, but dominates the phase diagram.

A final point should be made before finishing this section. As discussed in the Introduction, it has been shown[3,4] that linear rigid chain molecules of tangent hard segments exhibit liquid crystalline phase behavior for chain lengths equal to or larger than five segments. In particular, Vega *et al.*[4] have studied the phase behavior of the system with five tangent segments using *NPT* computer simulations. Following a compression route, they observed isotropic, nematic, smectic *A*, and solid phases. The hard system is related to the behavior of the LJ system at high temperatures (where the effect of attractions is small). Therefore, since linear rigid hard sphere chains form liquid crystals, one may expect that LJ linear rigid chains may also form liquid crystal phases (at least at high temperatures). However, in the simulations performed in this work for $m=5$ and $T^*=4$ in the fluid phase no evidence of liquid crystal phase formation was found. It remains to be considered if liquid crystal phases will appear for this model with $m=5$ at higher temperatures. De Miguel

and Vega[29] presented the global phase diagram of a Gay–Berne model system which includes solid, liquid crystalline, and fluid phases. In their chosen system a solid-nematic-fluid triple point is observed at relatively high temperature, and a second solid-liquid-vapor triple point is observed at low temperatures. We expect that a similar phase diagram may emerge for the system of linear rigid LJ molecules if high enough temperatures are studied; we will consider this point in future work.

IV. CONCLUSIONS

We have determined the global phase behavior (vapor-liquid and fluid-solid equilibria) of linear rigid chain molecules of three and five tangent LJ segments using computer simulations. The vapor-liquid equilibria were determined using Gibbs ensemble Monte Carlo simulations and isobaric-isothermal (*NPT*) calculations at zero pressure. In order to determine the fluid-solid coexistence densities at a given temperature, we obtained the free energies of each phase by thermodynamic integration. For the solid phase, this first required calculating the free energy at a particular (solid) state point. The Gibbs–Duhem integration technique was then used to obtain the solid-fluid transition at various temperatures. Zero-pressure *NPT* simulations have also been carried out at very low temperature to determine the coexistence solid densities along the sublimation curve. We have studied the effect of flexibility on the phase behavior by comparing the phase diagrams of flexible and rigid LJ chains.

The vapor-liquid critical conditions obtained in this work are found to be $T_c^*=2.081\pm0.016$, $P_c^*=0.060\pm0.017$, and $\rho_c^*=0.089\pm0.004$ for the linear rigid 3CLJ system, and $T_c^*=2.49\pm0.06$, $P_c^*=0.034\pm0.012$, and $\rho_c^*=0.046\pm0.009$ for the linear rigid 5CLJ system. In respect to the vapor-liquid coexistence, we find that flexible and rigid chains of LJ segments exhibit noticeable differences. This is a rather unexpected result, as the equation of state of linear and rigid chains of tangent hard segments are very similar.[18] The critical temperature of linear rigid LJ chains is found to be higher than that of flexible chains of corresponding chain length. In the limit of chains of infinite length, the difference is of about 25% (assuming the Schultz–Flory plot can be used for the short chains considered here).

As far as the fluid-solid phase equilibria are concerned, a clear stabilization of the solid phase with respect to the fluid is seen for increasing chain lengths; both the solid and fluid densities at coexistence (even when expressed in monomer units) shift toward lower densities for larger molecules. Together with this, a marked increase of the triple-point temperature is observed: the triple-point temperatures and densities for the linear rigid 3CLJ system are $T_t^*=1.040$, $\rho_l^*=0.281$, and $\rho_s^*=0.342$, while for the linear rigid 5CLJ system these are $T_t^*=2.050$, $\rho_l^*=0.122$, and $\rho_s^*=0.199$. As a result of the stabilization of the solid phase, the fluid range (given by the ratio T_t/T_c) decreases for increasing chain length, and it is predicted to disappear for chains with more than six tangent LJ segments. This is in marked contrast with the phase behavior predicted for systems of flexible LJ chains of tangent segments.[37] In the flexible molecular systems, the vapor-liquid coexistence was seen to dominate the phase diagram. To explain this one must take into account two factors. First, the equilibrium solid structure of fully flexible and linear rigid chains is completely different. Rigid linear chains freeze into an ordered arrangement of layers with all the molecules in a layer pointing in the same direction, while the stable solid structure of a system of fully flexible chains of tangent spherical segments is one with no long-range orientational order of bonds.

Second, the difference of the Hamiltonian does also affect the equation of state in the solid phase. It has been shown previously that even if a CP1 structure is ''imposed'' on a fully flexible chain in the solid phase, its equation of state differs from that of the rigid linear chain[41] in the same CP1 solid structure. Therefore the difference of the Hamiltonian affects the equation of state, even if the same solid structure is considered.

To summarize the content of this paper one may say that linear rigid LJ chains present a shrinkage of the liquid range, and that fully flexible LJ chains present a huge liquid range ($T_t/T_c=0.14$). The behavior of semiflexible molecular systems (such as *n*-alkanes) is expected to lie somewhere between these two extremes. In future work we plan to consider longer rigid chains and examine the phase behavior in more detail, analyzing the possibility of liquid crystal formation in these systems.

Note added in proof. Please note there was a misprint in Table I of Ref. 39. a_{ij} for $i=4$, $j=1$ should be 69.214 instead of 68.219 as reported.

ACKNOWLEDGMENTS

Financial support is due to Projects No. BFM-2001-1420-C02-01 and No. BFM-2001-1420-C02-02 of Spanish DGICYT (Dirección General de Investigación Científica y Técnica). A.G. would also like to thank the Engineering and Physical Sciences Research Council for the award of an Advanced Research Fellowship. E.S acknowledges the award of a FPU grant. L.G.M. acknowledges the award of a Ramon y Cajal grant. E.d.M. and F.J.B. would also like to thank Universidad de Huelva and Junta de Andalucía for additional financial support.

[1] Y. J. Sheng, A. Z. Panagiotopoulos, and S. K. Kumar, Macromolecules **29**, 4444 (1996).
[2] P. Paricaud, A. Galindo, and G. Jackson, Mol. Phys. **101**, 2575 (2003).
[3] D. C. Williamson and G. Jackson, J. Chem. Phys. **108**, 10 294 (1998).
[4] C. Vega, C. McBride, and L. G. MacDowell, J. Chem. Phys. **115**, 4203 (2001).
[5] R. Dickman and C. K. Hall, J. Chem. Phys. **85**, 4108 (1986).
[6] D. Frenkel, J. Phys. Chem. **92**, 3280 (1988).
[7] L. Onsager, Ann. N.Y. Acad. Sci. **51**, 627 (1949).
[8] G. J. Vroege and H. N. W. Lekkerkerker, Rep. Prog. Phys. **55**, 1241 (1992).
[9] H. Finewever and A. Yethiraj, J. Chem. Phys. **108**, 1636 (1998).
[10] M. R. Wilson, Mol. Phys. **81**, 675 (1994).
[11] M. S. Wertheim, J. Stat. Phys. **35**, 19 (1984).
[12] M. S. Wertheim, J. Stat. Phys. **35**, 35 (1984).
[13] M. S. Wertheim, J. Stat. Phys. **42**, 459 (1986).
[14] M. S. Wertheim, J. Stat. Phys. **42**, 477 (1986).
[15] M. S. Wertheim, J. Chem. Phys. **87**, 7323 (1987).
[16] W. G. Chapman, G. Jackson, and K. E. Gubbins, Mol. Phys. **65**, 1057 (1988).
[17] T. Boublík, C. Vega, and M. Diaz-Peña, J. Chem. Phys. **93**, 730 (1990).

[18] C. Vega, C. McBride, and L. G. MacDowell, Phys. Chem. Chem. Phys. **4**, 853 (2002).
[19] P. J. Flory, Proc. R. Soc. London, Ser. A **234**, 73 (1956).
[20] W. G. Chapmanf, J. Chem. Phys. **93**, 4299 (1990).
[21] J. K. Johnson, J. A. Zollweg, and K. E. Gubbins, Mol. Phys. **78**, 591 (1993).
[22] J. K. Johnson, E. A. Müller, and K. E. Gubbins, J. Phys. Chem. **98**, 6413 (1994).
[23] F. J. Blas and L. F. Vega, Mol. Phys. **92**, 135 (1997).
[24] L. A. Davies, A. Gil-Villegas, and G. Jackson, Int. J. Thermophys. **19**, 675 (1998).
[25] A. Gil-Villegas, A. Galindo, P. J. Whitehead, S. J. Mills, G. Jackson, and A. N. Burgess, J. Chem. Phys. **106**, 4168 (1997).
[26] L. A. Davies, A. Gil-Villegas, and G. Jackson, J. Chem. Phys. **111**, 8659 (1999).
[27] E. A. Müller and K. E. Gubbins, *Equations of State for Fluids and Fluid Mixtures* (Elsevier, Amsterdam, 2000).
[28] E. A. Müller and K. E. Gubbins, Ind. Eng. Chem. Res. **40**, 2193 (2001).
[29] E. de Miguel and C. Vega, J. Chem. Phys. **117**, 6313 (2002).
[30] I. A. Solov'yov, A. Solov'yov, W. Greiner, A. Koshelev, and A. Shutovich, Phys. Rev. Lett. **90**, 053401 (2003).
[31] Y. Zhou, M. Karplus, J. Wichert, and C. K. Hall, J. Chem. Phys. **107**, 10691 (1997).
[32] Y. Zhou, M. Karplus, K. D. Ball, and R. S. Berry, J. Chem. Phys. **116**, 2323 (2002).
[33] K. W. Wojciechowski, D. Frenkel, and A. C. Branka, Phys. Rev. Lett. **66**, 3168 (1991).
[34] K. W. Wojciechowski, A. C. Branka, and D. Frenkel, Physica A **196**, 519 (1993).
[35] C. Vega, E. P. A. Paras, and P. A. Monson, J. Chem. Phys. **96**, 9060 (1992).
[36] J. M. Polson and D. Frenkel, J. Chem. Phys. **109**, 318 (1998).
[37] C. Vega and L. G. MacDowell, J. Chem. Phys. **114**, 10411 (2001).
[38] C. McBride and C. Vega, J. Chem. Phys. **116**, 1757 (2002).
[39] C. Vega, F. J. Blas, and A. Galindo, J. Chem. Phys. **116**, 7645 (2002).
[40] C. Vega, C. McBride, E. de Miguel, F. J. Blas, and A. Galindo, J. Chem. Phys. **118**, 10696 (2003).
[41] E. Sanz, C. McBride, and C. Vega, Mol. Phys. **101**, 2241 (2003).
[42] H. C. Longuet-Higgins and B. Widom, Mol. Phys. **8**, 549 (1964).
[43] E. P. A. Paras, C. Vega, and P. A. Monson, Mol. Phys. **79**, 1063 (1993).
[44] F. J. Blas, A. Galindo, and C. Vega, Mol. Phys. **101**, 449 (2003).
[45] E. D. Nikitin, High Temp. **36**, 305 (1998).
[46] D. L. Morgan and R. Kobayashi, Fluid Phase Equilib. **63**, 317 (1991).
[47] C. Vega and C. McBride, Phys. Rev. E **65**, 052501 (2002).
[48] F. J. Blas, E. Sanz, C. Vega, and A. Galindo, J. Chem. Phys. **119**, 10958 (2003).
[49] V. A. Ivanov, M. R. Stukan, M. Müller, W. Paul, and K. Binder, J. Chem. Phys. **118**, 10333 (2003).
[50] M. P. Allen and D. J. Tildesley, *Computer Simulation of Liquids* (Clarendon, Oxford, 1987).
[51] G. S. Dubey, S. O'Shea, and P. A. Monson, Mol. Phys. **80**, 997 (1993).
[52] J. Stoll, J. Vrabec, H. Hasse, and J. Fischer, Fluid Phase Equilib. **179**, 339 (2001).
[53] F. J. Blas and L. F. Vega, J. Chem. Phys. **115**, 4355 (2001).
[54] A. Z. Panagiotopoulos, Mol. Phys. **61**, 813 (1987).
[55] F. A. Escobedo and J. J. de Pablo, Mol. Phys. **87**, 347 (1996).
[56] Y. J. Sheng, A. Z. Panagiotopoulos, S. K. Kumar, and I. Szleifer, Macromolecules **27**, 400 (1994).
[57] A. Perera and F. Sokolic, Mol. Phys. **88**, 543 (1996).
[58] C. Vega, E. P. A. Paras, and P. A. Monson, J. Chem. Phys. **97**, 8543 (1992).
[59] M. Parrinello and A. Rahman, Phys. Rev. Lett. **45**, 1196 (1980).
[60] S. Yashonath and C. N. R. Rao, Mol. Phys. **54**, 245 (1985).
[61] D. Frenkel and A. J. C. Ladd, J. Chem. Phys. **81**, 3188 (1984).
[62] M. A. van der Hoef, J. Chem. Phys. **113**, 8142 (2000).
[63] R. Agrawal and D. A. Kofke, Mol. Phys. **85**, 43 (1985).
[64] A. R. Schultz and P. J. Flory, J. Am. Chem. Soc. **74**, 7460 (1952).